Oscillations in harmonics generated by the interaction of acoustic beams

Mark D. Cahill and Andrew C. Baker[a)]
Department of Physics, University of Bath, Bath BA2 7AY, United Kingdom

(Received 4 August 1997; revised 12 November 1998; accepted 14 November 1998)

A numerical model of nonlinear propagation is used to investigate two cases of monochromatic ultrasonic beams interacting at small angles in a nonlinear medium. Two finite Young's slits are seen to produce fringes at harmonic frequencies of the source in places where the source frequency is absent, which can be seen as a combination of harmonic generation near the source, and in the beam. Two intersecting beams with shaded edges are seen to produce similar fringes in the near field, with an oscillatory structure. Algebraic solutions to a simplified model, using the weak-field Khokhlov–Zabolotskaya equation, are invoked to illustrate the origin of the oscillations, and of the far-field directivity, providing an alternative view of the fringes due to Young's slits. It is seen that two weakly interacting beams can produce fringes of second harmonic where the source frequency has low amplitude, if the beams coincide at the point of observation, or if a boundary condition is imposed on the second harmonic where the beams coincide. © *1999 Acoustical Society of America.* [S0001-4966(99)03103-3]

PACS numbers: 43.25.Cb, 43.25.Jh [MAB]

INTRODUCTION

It has been established that when a sound wave of finite amplitude passes through a nonlinear medium, the wave tends to steepen in such a way as to produce harmonics of the source frequency, and for the case of waves whose components are approximately collinear, the Khokhlov–Zabolotskaya–Kuznetsov (KZK) equation[1] has been found to describe this phenomenon. This equation has been shown to possess solutions which exhibit what have come to be known as ''fingers''[2]—fringes at harmonic frequencies, which appear between the regions of constructive interference in the source frequency, and these have been observed experimentally.[3,4]

What might be considered surprising about this phenomenon is the assumption that, since (in a first approximation) harmonics are necessarily generated where the fundamental is nonzero, and since the harmonics due to the self-action of a plane wave have motion parallel to that wave, then the harmonic fringes should in some sense follow those of the source frequency. This is compounded by the observation of Westervelt[5] that the wave equation which he derived, and to which the KZK equation approximates in the case of near-collinearity, a nondissipative medium, and weak nonlinearity,[6] possesses a solution which is proportional to a quantity (related to the energy density) quadratic in the fundamental beam, and which thus vanishes where the fundamental and its derivatives vanish. A similar conclusion is reached by Jiang and Greenleaf[7] for a dissipative medium.

Many studies have been published which show that fingers nevertheless do appear (see also, for example, Refs. 6 and 8), and the purpose of this paper is to elucidate the mechanisms of their production by means of two simple, if idealized, examples. In the process, the phenomenon of oscillation[9] of harmonics is explored, and seen to be both a cause of fingers in the near field, and a limiting factor on those in the far field.

The KZK equation,

$$\frac{\partial^2 p'}{\partial\sigma\,\partial\tau}=\alpha r_0\frac{\partial^3 p'}{\partial\tau^3}+\frac{1}{4}\nabla_\perp^2 p'+\frac{r_0}{2l_d}\frac{\partial^2 p'^2}{\partial\tau^2}, \tag{1}$$

assumes that the beam can be regarded as propagating approximately in one direction, along the z axis, in the absence of vorticity.

It is most convenient to perform the general analysis in terms of dimensionless quantities; τ is the dimensionless retarded time coordinate

$$\tau=\omega t-kz, \tag{2}$$

p' is a dimensionless measure of the overpressure,

$$p'=(P-p_0)/P_0, \tag{3}$$

P being the pressure, p_0 is the ambient pressure, and P_0 is here taken to be the amplitude of the pressure at the source, and the wave has a characteristic wavelength $\lambda=2\pi/k$, frequency $f=\omega/2\pi$, and speed c (the medium is assumed nondispersive). The Rayleigh distance,

$$r_0=\pi a^2/\lambda, \tag{4}$$

where a is a characteristic radius of the beam near the source, is itself a characteristic distance in the direction of propagation, and defines the dimensionless coordinate

$$\sigma=\frac{z}{r_0}. \tag{5}$$

The first term on the rhs is the absorption, with coefficient

$$\alpha=\alpha_0 f^2, \tag{6}$$

[a)]Now working at Christian Michelsen Research AS, Fantoftvegen 38, Postboks 6031, 5020 Bergen, Norway.

 0001-4966/99/105(3)/1575/9/$15.00

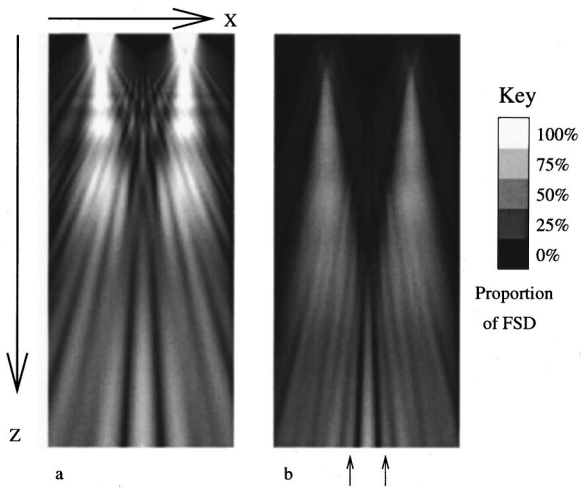

FIG. 1. Amplitude plot of Young's fringes, showing a region 33 mm wide, the beams propagating down the page for 150 mm. The images are expanded ×2 horizontally. (a) Fundamental, full scale deflection (FSD)=1 MPa, (b) second harmonic, FSD=0.5 MPa. Two fingers are indicated by arrows.

$$\alpha_0 = 2.5\times 10^{-14}\ \ \mathrm{Np\,m^{-1}\,Hz^{-2}} \tag{7}$$

in water, the second term is diffraction, with

$$\nabla_{\perp}^2 = \frac{\partial^2}{\partial x'^2} + \frac{\partial^2}{\partial y'^2}, \tag{8}$$

$$(x',y') = (x,y)/a, \tag{9}$$

and the last term describes the nonlinear distortion, with the ''shock wave formation distance''

$$l_d = \frac{c^2\rho_0}{\beta k P_0} \tag{10}$$

the approximate distance at which, neglecting attenuation, a plane wave of given amplitude forms a shock wave, β being 3.5 in water.

The numerical tool used to solve this is the Bergen code,[10,11] which solves the KZK equation as a set of diffusion equations, one for each temporal harmonic of the beam, weakly coupled by the nonlinear term. This is done using finite difference algorithms and with coordinates appropriate to a spherically diverging beam.

I. NUMERICAL RUNS

Specific examples of acoustic interactions are given in the following sections, and specific dimensional parameters are given. These can be related to the dimensionless quantities of the general equations by Eqs. (2)–(10).

A. Young's slits

Figure 1(a) shows the fundamental beam due to two slits of width 5 mm and length 20 mm, separated by 10 mm, the beam propagating down the page, through water for a distance of 150 mm. The image is a cross section through the center of the beam, perpendicular to the slits, and one sees the usual fringes fanning out towards the bottom of the image. The amplitude of the initial wave, P_0 is 1 MPa, and the frequency is 2.25 MHz, under which conditions the system is strongly nonlinear, so that in addition to the fringes of the fundamental, one also sees fringes at harmonic frequencies. Figure 1(b) is the second harmonic field produced by the nonlinear interaction. In addition to the second harmonic seen within each fringe of the fundamental, it also clearly possesses ''fingers'' between these fringes. This is hardly surprising, since we see that in the region just below the slits, the fundamental possesses maxima, which are effectively sources of the second harmonic. Two such sources might be expected to produce an interference pattern with twice the transverse spatial frequency found in the fundamental, simply because the second harmonic has half of the wavelength of the fundamental. From this oversimplified point of view, then, the fingers are the result not of nonlinear interaction of the beams, one from each slit, but of the superposition of the beams, each with its compliment of the second harmonic, and higher harmonics, produced prior to the interaction.

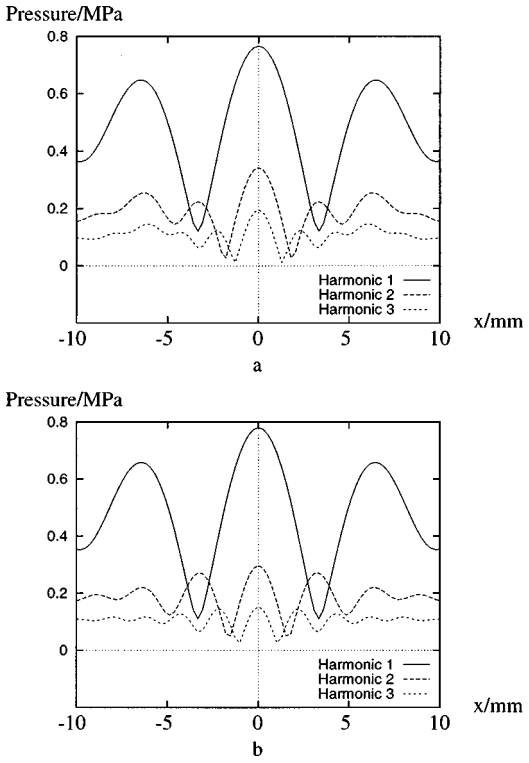

FIG. 2. Amplitude of the first three harmonic components in a cross section of the beam from Young's slits, corresponding to the bottom of Fig. 1: (a) fully interacting field and (b) field due to each slit separately calculated and then superposed.

Figure 2(a) shows a cross section of the beam at $z=150\,\mathrm{mm}$, $y=0$, i.e., across the bottom of the images. It includes the third harmonic, which also shows fringes; for each fringe of the fundamental there are two corresponding fringes of the second harmonic, and three of the third, just as would be expected from a superposition of two noninteracting sources. Figure 2(b), however, shows the pattern produced by adding the fields of two such noninteracting slits, calculated using the same model. The two patterns are very similar, but there is a visible difference—the interacting beams have slightly stronger second and third harmonic fringes where there is a fundamental fringe, and the fingers (located at the fundamental minima) are slightly diminished.

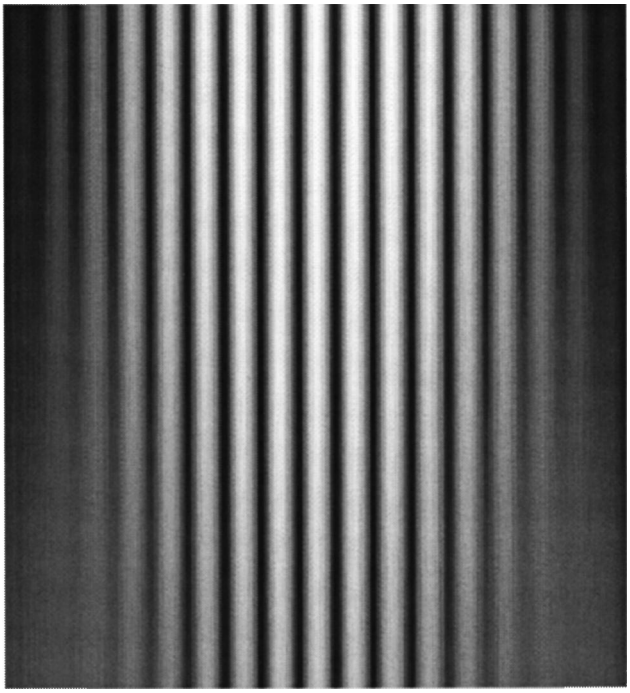

FIG. 3. Fundamental amplitude due to cosine grating (intersecting beams) in plane $y=0$. Beam propagates down the page from grating at the top. FSD=1 MPa. Region shown is 67 by 150 mm^2, expanded $\times 2$ horizontally.

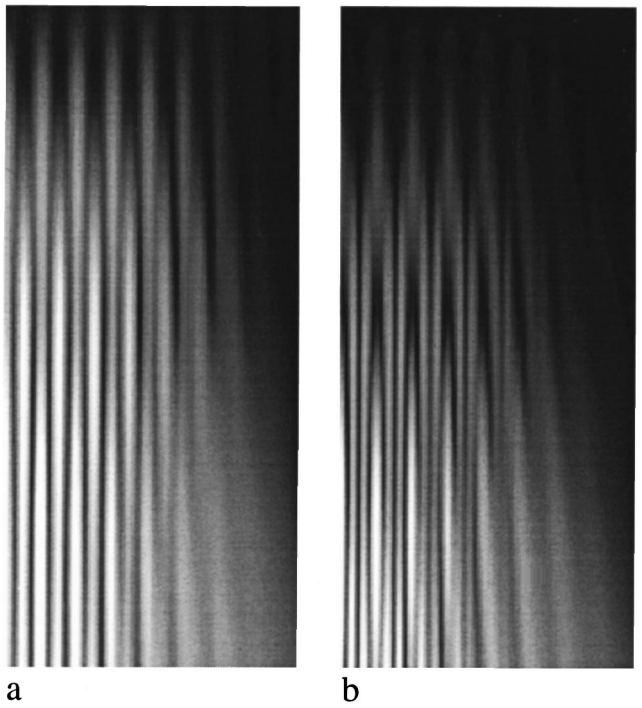

FIG. 4. Amplitude plots for cosine grating (intersecting beams), as in Fig. 3, but for (a) second harmonic, FSD=0.25 MPa and (b) third harmonic, FSD=0.167 Mpa. Beam propagates down the page from grating at the top, with the top left-hand corner being at the center of the source. Region shown is 33 by 150 mm^2, expanded $\times 2$ horizontally.

The nonlinear interaction of the beams acts to *diminish* the fingers. This also is not surprising, if we consider that some of the harmonic generation will take place where the beams are interacting, so that there will be increased generation of harmonics where there is constructive interference of the fundamental, and where there is destructive interference of the fundamental there will be less harmonic generation, than in the case of the noninteracting slits. It is known[2] that for a circular source the fingers diminish as $1/r$, while the lobes corresponding to those of the fundamental diminish more slowly, as $\ln(r)/r$, being continuously ''pumped'' by the (itself diminishing) fundamental.

B. Cosine grating

While Young's slits are a familiar system, their spatial spectrum still has a complex structure, making it difficult to see clearly the spatial properties of harmonic generation. A simpler system is now considered in which the interacting beams cross at the origin and possess shaded edges, which limit the width of their spatial spectra. The source function

$$p' = \cos(Kx') f(x',y') \tag{11}$$

for $K>10$ has a spatial spectrum in the x direction with two clearly defined lobes, at $k_x = \pm K/a$, for a reasonably smooth $f(x',y')$, that is, it represents two beams crossing at an angle

$$2\theta = \frac{2K}{ka}. \tag{12}$$

First consider the case

$$f(x',y') = \exp(-5(x'^2+y'^2)^2), \tag{13}$$

which is flatter than a Gaussian profile, and take $K=10\pi$, the pressure $P_0=1$ MPa, frequency $f=2.25$ MHz, and dimension of the source $a=4$ cm.

Figure 3 shows the resulting evolution of the fundamental in the near field, as it propagates 15 cm down the page, from the grating at the top of the figure, in the plane $y'=0$, perpendicular to the grating. Across the top the source falls off, while down the page at the sides, the fringes become less distinct as the two beams separate. Figure 4(a) shows the second harmonic. The left half of the image has been cut off, so that the top left-hand corner corresponds to the center of the grating, but the scale is the same as in Fig. 3. As the beam propagates downwards, fringes of second harmonic appear, as expected, where the fundamental has the greatest amplitude. At 4 cm from the source, however, fingers start to appear between these principal fringes, and at 8 cm from the source these fingers are brighter than the principal fringes. Figure 4(b) shows the same thing occurring in the third harmonic—principal fringes appear at the maxima of the fundamental, to be outshone by two intermediate fingers 7 cm from the source. The oscillations continue, with the principal fringes brightest 11 cm from the source, and (just discernibly) the fingers brightest at the bottom of the image.

To see what is happening here, consider Fig. 5. This shows the spatial spectrum of the second harmonic (in the x direction, for $y=0$), from Fig. 4(a), as a function of z, the beam propagating into the page. To the right of the figure is a band with spatial frequency twice that of the fundamental. This grows smoothly, as might be expected. To the left, however, is a band centered on $k_t=0$ which, while initially grow-

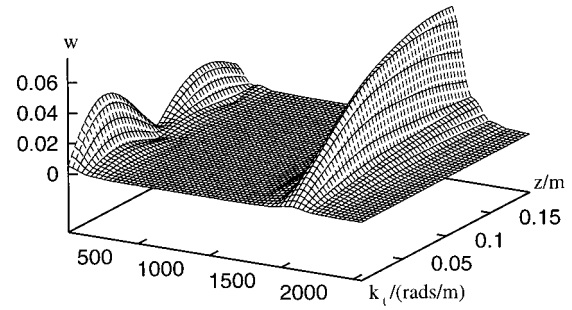

FIG. 5. Amplitude of the transverse Fourier transform of the second harmonic, as a function of z, the distance from a cosine grating. The units of k_t are rad/m, the fundamental having a maximum at $k_t = K/a = 785$ rad/m, which generates second harmonic components at $\pm K/a \pm K/a$.

ing twice as fast as the right-hand band, proceeds to oscillate. The initial behavior is what one might expect, since the self-action of each component of the fundamental (at $k_t = \pm K/a$) will create the right-hand bands, and the interaction of the two will create one with zero spatial frequency, and will be seen in some sense to be associated with the fingers.

Oscillations have been noted before in harmonic generation,[9,12] where they were seen to be due to beating between the generated harmonic field and the field due to the boundary conditions, and this will be seen to be the case here as well.

II. ANALYSIS

A. The weak-field approximation

The previous example involved a strong field, in a dissipative medium. In order to gain a clearer understanding of the origin of the oscillations in Figs. 4 and 5, consider Eq. (1) in the limit of negligible absorption, α, and adopt the quasi-linear approximation, in which we need only consider fields due to the self-action of the fundamental field.

Equation (1) becomes the Khokhlov–Zabolotskaya (KZ) equation

$$\frac{\partial^2 p'}{\partial\sigma\,\partial\tau} = \frac{1}{4}\nabla_\perp^2 p' + \frac{r_0}{2l_d}\frac{\partial^2 p'^2}{\partial\tau^2}, \tag{14}$$

and, adopting the Fourier decomposition

$$p' = \frac{1}{2i}\sum_{n=-\infty}^{\infty} W_n(x',\sigma)e^{in\tau}, \tag{15}$$

$$W_n = -W_{-n}^*, \tag{16}$$

$$W_0 = 0 \tag{17}$$

(the normalization is appropriate to the computer program), we find

$$\frac{\partial W_n(\sigma)}{\partial\sigma} = -\frac{i}{4n}\nabla_\perp^2 W_n + \frac{r_0 n}{4l_d}\sum_{m=-\infty}^{\infty} W_{n-m}W_m. \tag{18}$$

If the source includes only the fundamental W_1, with

$$W_1(x',0) = \cos(Kx')\exp(-2x'^2), \tag{19}$$

independent of y, then in the quasi-linear approximation,[2]

$$\frac{\partial W_1(x',\sigma)}{\partial\sigma} = -\frac{i}{4}\frac{\partial^2 W_1}{\partial x'^2}, \tag{20}$$

$$\frac{\partial W_2(x',\sigma)}{\partial\sigma} = -\frac{i}{8}\frac{\partial^2 W_2}{\partial x'^2} + \frac{r_0}{2l_d}W_1^2. \tag{21}$$

Decomposing W_n into its transverse spatial spectrum,

$$W_n(x',\sigma) = \int_{-\infty}^{\infty} e^{-ik_x x'}\omega_n(k_x,\sigma)dk_x, \tag{22}$$

then

$$\frac{\partial\omega_1(k_x,\sigma)}{\partial\sigma} = \frac{ik_x^2}{4}\omega_1(k_x,\sigma), \tag{23}$$

$$\frac{\partial\omega_2(k_x,\sigma)}{\partial\sigma} = \frac{ik_x^2}{8}\omega_2(k_x,\sigma) + \frac{r_0}{2l_d}\int_{-\infty}^{\infty}\omega_1(k_x-k_x',\sigma)\omega_1(k_x',\sigma)dk_x', \tag{24}$$

and

$$\omega_1(k_x,0) = \sqrt{\frac{1}{32\pi}}\left[\exp\left(-\frac{(k_x+K)^2}{8}\right) + \exp\left(-\frac{(k_x-K)^2}{8}\right)\right], \tag{25}$$

so that

$$\omega_1(k_x,\sigma) = \sqrt{\frac{1}{32\pi}}\left[\exp\left(-\frac{(k_x+K)^2}{8}\right) + \exp\left(-\frac{(k_x-K)^2}{8}\right)\right]\exp(ik_x^2\sigma/4), \tag{26}$$

which has the inverse transform

$$W_1(x',\sigma) = \frac{1}{2\sqrt{1-2i\sigma}}\left[\exp\left(\frac{(4ix'+K)^2}{8(1-2i\sigma)} - \frac{K^2}{8}\right) + \exp\left(\frac{(4ix'-K)^2}{8(1-2i\sigma)} - \frac{K^2}{8}\right)\right]. \tag{27}$$

The two terms in the square brackets are clearly the two diverging beams, whose amplitudes at $x' = \mp K\sigma/2$, decrease as $1/\sqrt[4]{1+4\sigma^2}$. The wave is described in Eq. (1) with a retarded time coordinate, so the greater part of the phase of each component is implicit in the representation; however, the first terms on the rhs of the differential equations (23) and (24) impose a phase lag on the wave due to its having a component in the transverse (x) direction, proportional to the square of k_x. This is due to the relation $\mathbf{k}^2 = \omega^2/c^2$, $\mathbf{k}$ and ω being the dimensional angular frequencies, in the parabolic approximation $k_x \ll 1$ [see the discussion introducing Eq. (1)].

B. Near-field oscillations

Now applying Eq. (26) to Eq. (24), and evaluating the convolution, one finds

$$\frac{\partial\omega_2(k_x,\sigma)}{\partial\sigma}=\frac{ik_x^2}{8}\omega_2(k_x,\sigma)+\frac{r_0}{32l_d\sqrt{\pi(1-2i\sigma)}}\times\left[\exp\left(-\frac{(k_x+2K)^2}{16}\right)+\exp\left(-\frac{(k_x-2K)^2}{16}\right)+2\exp\left(-\frac{k_x^2}{16}+\frac{iK^2\sigma}{2(1-2i\sigma)}\right)\right]e^{ik_x^2\sigma/8}, \tag{28}$$

which, confining attention for now to the region near the grating with

$$K^2\sigma^2\ll 1,\quad \sigma\ll 1, \tag{29}$$

is

$$\frac{\partial\omega_2(k_x,\sigma)}{\partial\sigma}\approx\frac{ik_x^2}{8}\omega_2(k_x,\sigma)+\frac{r_0}{32\sqrt{\pi}l_d}\times\left[\exp\left(-\frac{(k_x+2K)^2}{16}\right)+\exp\left(-\frac{(k_x-2K)^2}{16}\right)+2\exp\left(-\frac{k_x^2}{16}+\frac{iK^2\sigma}{2}\right)\right]e^{ik_x^2\sigma/8}. \tag{30}$$

All three components in the square brackets represent Gaussians with greater width than those in Eq. (26), corresponding in configuration space to a source narrower than the width of the fundamental. The first two terms are due to the convolution of each term of Eq. (26) with itself, and are centered on $k_x=\mp 2K$, with a phase lag $ik_x^2\sigma/8$, as might be expected, but the third, which is due to the convolution of each beam with the other, and so represents the interaction of the two, while centered on $k_x=0$, has an additional phase lag $iK^2\sigma/2$. This additional lag is directly attributable to that in the beams of the fundamental, which each possess a lag appropriate to a mode with $k_x=K$, and it is this which can be seen as the cause of the oscillations.

Imposing the condition that there is no second harmonic at the grating

$$\omega_2(k_x,0)=0, \tag{31}$$

Eq. (30) has the solution

$$\omega_2(k_x,\sigma)\approx\frac{r_0}{32l_d\sqrt{\pi}}\left[\left(\exp\left(-\frac{(k_x+2K)^2}{16}\right)+\exp\left(-\frac{(k_x-2K)^2}{16}\right)\right)\sigma+\frac{4i}{K^2}(1-e^{iK^2\sigma/2})\exp\left(-\frac{k_x^2}{16}\right)\right]e^{ik_x^2\sigma/8}. \tag{32}$$

In configuration space, and given the approximation (29), this is

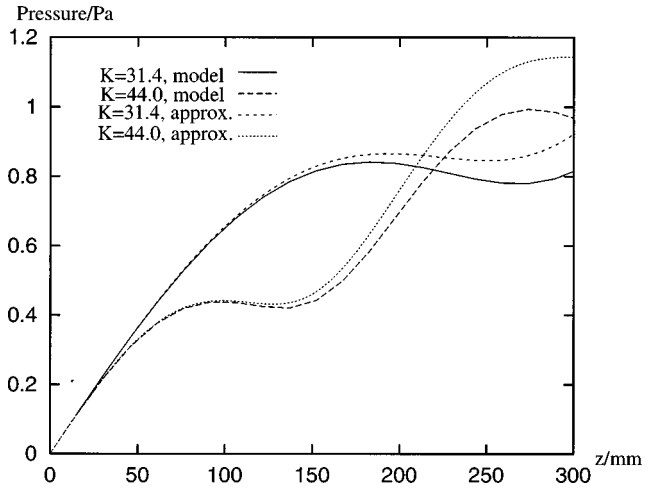

FIG. 6. Comparison of predictions from the numerical model, and from the algebraic approximation equation (33), for the axial variation of the amplitude of the second harmonic, for $K=10\pi$ and $K=14\pi$.

$$W_2(x',\sigma)\approx\frac{r_0}{8l_d}e^{-4x'^2}\left[2e^{iK^2\sigma/2}\cos(2Kx')\sigma+\frac{8}{K^2}e^{iK^2\sigma/4}\sin\left(\frac{K^2\sigma}{4}\right)\right]. \tag{33}$$

Figures 6 and 7 compare this approximation with the results of model runs. Here a is taken as 8 cm, the (ideally infinite) length of the slits is taken to be 80 cm, $\alpha=0$, $P_0=1$ kPa, and all other parameters are as before. Figure 6 shows the amplitude of the beam along the central lobe $(x'=0)$ for two values of K, while Fig. 7 compares the complex components for $K=10\pi$. While the approximation becomes invalid after a couple of cycles, it reproduces the oscillations and phase variation of the first cycle well.

The first two terms in the square brackets of Eq. (32) vary as σ, while the third oscillates, being proportional to $(1-e^{iK^2\sigma/2})$. This is the difference between a component generated in the beam, which rotates in phase due to the lag $iK^2\sigma/2$ mentioned above, and a term due to the boundary

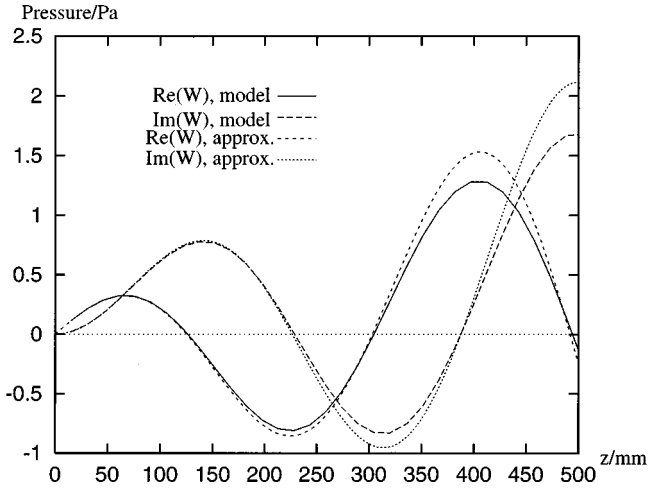

FIG. 7. Comparison of predictions by the numerical model, and by the algebraic approximation equation (33), for the axial variation of the complex components of the second harmonic. $K=10\pi$.

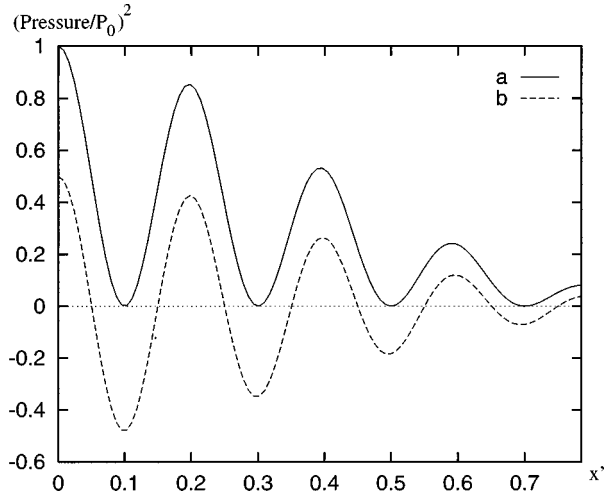

FIG. 8. Illustrating a mechanism for the production of fingers; (a) the square of the source function $W_1(x',0)$, for $K=10\pi$, to which the second harmonic is initially proportional and (b) the same function with an offset of half the envelope $\exp(4x'^2)$. (b) Posesses fingers at $x'=0.1, 0.3,\ldots$.

condition (31), which propagates with the natural phase. These interfere to produce the sine in the second term of Eq. (33), and describe an oscillation like that seen in Fig. 5.

Regarding the production of fingers, for very small $K^2\sigma$, the coefficient of the third Gaussian (the cross term) in Eq. (32) is approximately 2σ, so that

$$\omega_2(k_x,\sigma)\approx\frac{r_0\sigma}{32l_d\sqrt{\pi}}\left[\left(\exp\left(-\frac{(k_x+2K)^2}{16}\right)+\exp\left(-\frac{(k_x-2K)^2}{16}\right)\right)+2\exp\left(-\frac{k_x^2}{16}\right)\right], \tag{34}$$

which, up to a Gaussian envelope, is the Fourier transform of $\cos^2(Kx')$ [see Eq. (19)], which has zero amplitude where W_1 is zero. By $\sigma=2\pi/K^2$, however, the coefficient of the cross term is zero (the field due to the boundary condition cancels that generated by the beam), and Eq. (32) then resembles the Fourier transform of $\cos(2Kx')$. The situation is illustrated by Fig. 8; the cross term is proportional to the envelope (being centered about $k_x=0$), and its cancellation produces a field with negative values where there is no fundamental field, which are the fingers.

C. Fingers in the far field

An exact solution to the perturbative cosine grating will now be found, which will reveal another mechanism, by which the $k_x=0$ component can manifest itself as a single finger, rather than the multiple fingers seen in the near field. Instead of using inequalities (29), write the solution to Eq. (28) in integral form as

$$\omega_2(k_x,\sigma)=e^{ik_x^2\sigma/8}\frac{r_0}{32l_d\sqrt{\pi}}\int_{\sigma_0}^{\sigma}\frac{d\sigma'}{\sqrt{1-2i\sigma'}}\times\left[\exp\left(-\frac{(k_x+2K)^2}{16}\right)+\exp\left(-\frac{(k_x-2K)^2}{16}\right)+2\exp\left(-\frac{k_x^2}{16}+\frac{iK^2\sigma'}{2(1-2i\sigma')}\right)\right], \tag{35}$$

where the lower bound of the integration σ_0 will be set to 0 at the end of the calculation, to implement the boundary condition equation (31). Delaying the evaluation of this until after the inverse Fourier transform has been performed,

$$W_2(x',\sigma)=\frac{r_0}{8l_d\sqrt{1-2i\sigma}}\int_{\sigma_0}^{\sigma}\frac{d\sigma'}{\sqrt{1-2i\sigma'}}\times\left[\exp\left(\frac{(4ix'+K)^2}{4(1-2i\sigma)}-\frac{K^2}{4}\right)+\exp\left(\frac{(4ix'-K)^2}{4(1-2i\sigma)}-\frac{K^2}{4}\right)+2\exp\left(-\frac{4x'^2}{1-2i\sigma}+\frac{K^2}{4}\left(\frac{1}{1-2i\sigma'}-1\right)\right)\right], \tag{36}$$

we eventually find

$$W_2(x',\sigma)=\frac{r_0}{8l_d}\left\{\frac{i}{\sqrt{1-2i\sigma}}(\sqrt{1-2i\sigma}-\sqrt{1-2i\sigma_0})\times\left[\exp\left(\frac{(4ix'+K)^2}{4(1-2i\sigma)}-\frac{K^2}{4}\right)+\exp\left(\frac{(4ix'-K)^2}{4(1-2i\sigma)}-\frac{K^2}{4}\right)\right]+\mathrm{cr}(K,x',\sigma,\sigma_0)-\mathrm{cr}(K,x',\sigma,\sigma)\right\}, \tag{37}$$

where the function cr, due to the cross term, is

$$\mathrm{cr}(K,x',\sigma,\tau)=\frac{K}{\sqrt{1-2i\sigma}}\exp\left(-\frac{4x'^2}{1-2i\sigma}-\frac{K^2}{4}\right)\times\left[\frac{2\sqrt{1-2i\tau}}{iK}\exp\left(\frac{K^2}{4(1-2i\tau)}\right)+\sqrt{\pi}\,\mathrm{erf}\left(\frac{iK}{2\sqrt{1-2i\tau}}\right)\right], \tag{38}$$

and

$$\mathrm{erf}(y)=\frac{2}{\sqrt{\pi}}\int_0^y\exp(-y'^2)dy'. \tag{39}$$

The terms other than the cross term in Eq. (37) are the self-action of each beam. Note that for finite σ_0, $x'=\mp K\sigma/2$, large σ, they tend to a constant—decreased amplitude as the beam spreads is cancelled by growth due to generation from

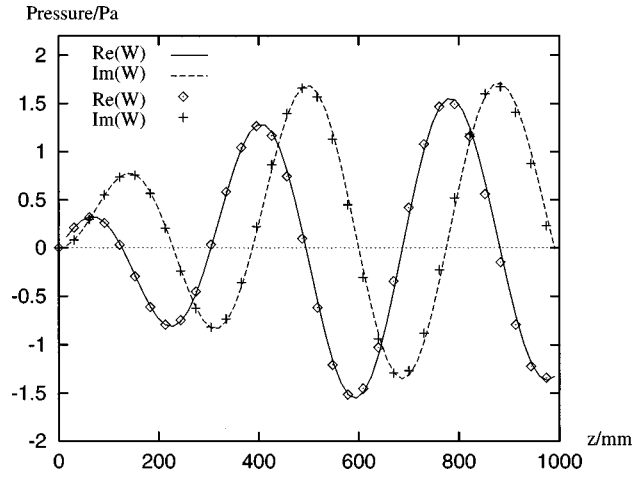

FIG. 9. Comparison of predictions by the numerical model (curves), and by the exact solution equation (37) (points), for the axial variation of the complex components of the second harmonic. $K=10\pi$, $P_0=1$ kPa.

the fundamental. The analogous behavior for a three-dimensional problem is $\omega_2 \sim \ln(z)/z$,[2] as noted at the end of Sec. I A.

While Eq. (37) is not easy to evaluate, packages such as Maple are quite capable of tabulating and plotting it. Figure 9 compares the axial behavior of the exact solution, with the model run of Figs. 6 and 7, and Fig. 10 compares them in a cross section of the beam 274 mm from the grating, a point where the fingers are stronger than the principal fringes. The slight deviation of the model from theory for large z in Fig. 9 may be due to the finite length of the slits in the model run. Otherwise, the fit is exact enough to confirm the accuracy of the Bergen code, and incidentally to reassure one that the algebra is correct.

Turning to the cross term,

$$\mathrm{cr}(K,x',\sigma,\sigma)-\mathrm{cr}(K,x',\sigma,\sigma_0), \tag{40}$$

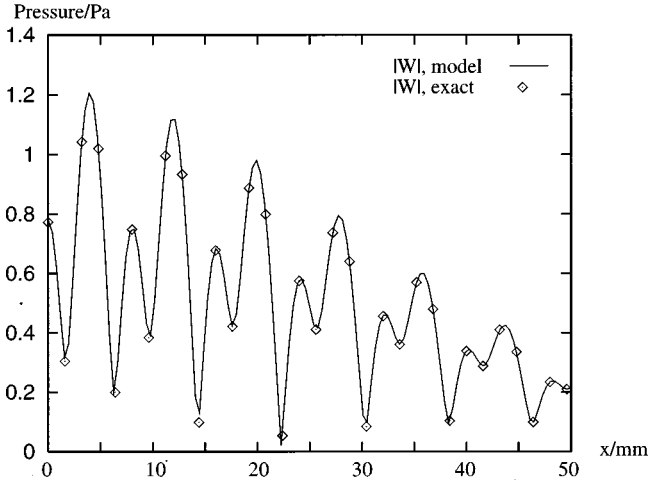

FIG. 10. Comparison of predictions by the numerical model (curves), and by the exact solution equation (37) (points), for the transverse variation of the magnitude of the second harmonic at $z=274$ mm. Note that the fingers are stronger than the principal fringes. $K=10\pi$, $P_0=1$ kPa.

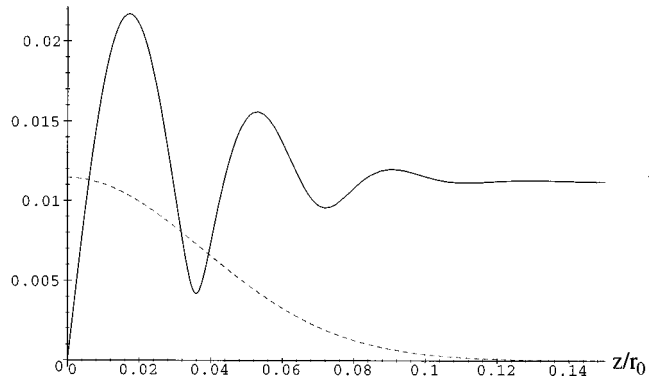

FIG. 11. Amplitude of the cross-term equation (40), on axis ($x=0$) for $K=6\pi$: boundary condition equations (31) (continuous line) and (41) (dashed line).

for very large σ (finite x' and σ_0) this tends to $-2i\times\exp(-K^2/4)$, which is to say that there is a constant term in the limit proportional to the overlap of the directivities of the beams. Insofar, then, as the fundamental beams propagate in different directions, this limit is negligible. Setting $\sigma_0=0$, in accord with Eq. (31), the continuous line in Fig. 11 shows that the amplitude of the term oscillates at first, then settles down to an almost constant value for moderate values of σ, eventually falling off as $1/\sqrt[4]{1+4\sigma^2}$. As the principal fringes diverge, this term propagates down the z axis, to form a finger.

The solution (27) is defined for negative σ, and while it would be difficult to create such a beam, it is still meaningful to ask what second harmonic field it would generate, if the second harmonic were set to zero at some point before the intersection of the beams. With this in mind, the dashed line in Fig. 11 shows the amplitude of the cross term assuming

$$\omega_2(k_x,-10)=0, \tag{41}$$

i.e., with $\sigma_0=-10$. With this boundary condition, the second harmonic is effectively zero outside the region in which both fundamental beams are present—just the behavior described by Westervelt. To see how these two cases differ, consider Figs. 12 and 13, which show the complex components of the cross term for each boundary condition. In the ''Westervelt'' case, Fig. 12, there is a substantial imaginary component of the second harmonic at the origin. In order to

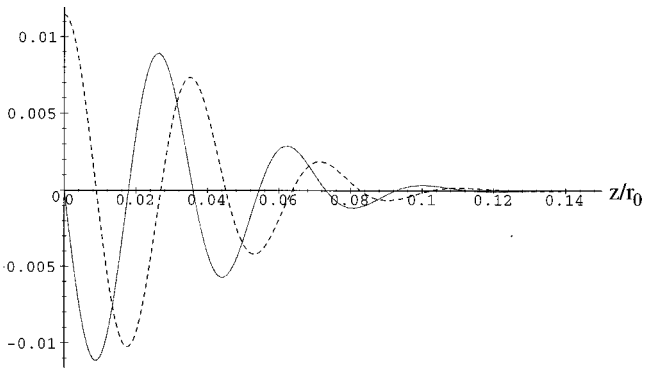

FIG. 12. Axial components of the cross term for boundary condition equation (41): real component (continuous line) and imaginary component (dashed line).

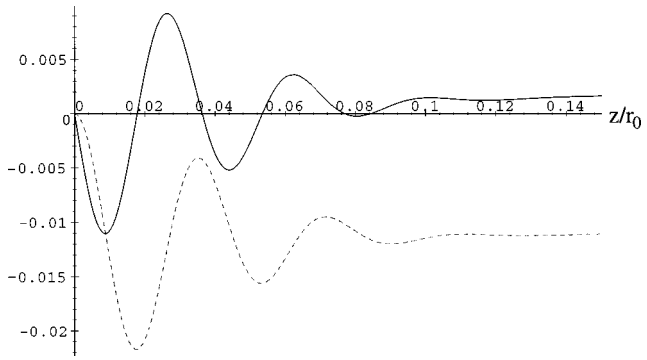

FIG. 13. Axial components of the cross term for boundary condition equation (31): real component (continuous line) and imaginary component (dashed line).

set this to zero for the boundary condition at $\sigma_0=0$, a component must be subtracted, whose evolution is seen in Fig. 13 to produce a large negative imaginary component beyond the region of interaction of the beams [which slowly rotates into the real component due to the factor $1/\sqrt{1-2i\sigma}$ in Eq. (38)]. The far-field finger is thus seen to be a direct result of the boundary condition, Eq. (31). It is the ''free wave'' of Naze Tjøtta and Tjøtta.[9]

III. DISCUSSION

It has been seen in the previous two sections that the development of fingers in the near and far fields of a simple system can be attributed to the difference between the spatial frequencies of freely propagating waves of the second harmonic, and of the source function due to the interaction of noncollinear beams. In the near field, the mismatch causes this component to stop growing, as it becomes out of phase with its source, which shifts the fringe pattern to produce fingers of opposite phase. In the far field, this mismatch can be seen as the reason that the generated component (the ''Westervelt component'') does not propagate beyond the region of interaction of the beams—it is a commonplace result of scattering theory that ''off-shell'' modes, i.e., modes which do not satisfy the free-field equation, do not propagate (see Ref. 13, Chap. 5, Sec. 2), and the fact that the phase of the source function rotates with respect to a free field propagating in the same direction indicates that it is the source of an off-shell field. The component which cancels this off-shell field at the boundary, however, is itself on-shell, and it is this which propagates. The effect of boundary conditions on generated harmonics was explored more fully in Refs. 14 and 15. On the other hand, components of the two beams which are collinear produce a source field which is on-shell, and so generates a component of the second harmonic which propagates.

The objection might rightly be raised that by imposing the boundary condition equation (19), appropriate to a source, and then considering the beams as originating before that point, one is describing an artificially symmetrical arrangement, which might not be representative of more realistic systems. Fortunately, Darvennes and Hamilton[16] have considered a system in which the boundary conditions possess two distinct Gaussian sources in three dimensions, whose beams then cross, subject to the KZ equation. Their Eq. (24), describing the far-field behavior, contains two terms, one proportional to the product of the directivities of the source, and varying as $\ln(z)/z$ [the counterpart of the constant limit $-2i\exp(-K^2/4)$ above], due to collinear components in the beams, and the other a bilinear function of the beams at the boundary, as must the ''free field'' component be, if at the boundary it is to cancel the Westervelt component, itself bilinear in the fundamental beams.

Finally, to revisit the Young's fringes, although Figs. 1 and 2 refer to beams with finite amplitude and absorption, one can envisage the second harmonic in a low-amplitude system as being composed of three fields—the first generated by the interaction of collinear modes in the two beams, the second due to the local interaction of noncollinear modes (bearing in mind that the beams overlap through most of the half-space $z>0$), and the third attributable to the boundary condition, which requires cancellation at $z=0$ of the field generated by local interaction of the fundamental field. In practice, however, the distinction between these is ambiguous, both because it depends on the choice of boundary, and because sources of modes which violate only slightly the free-field equation must act for a considerable distance before drifting out of phase with their generated waves. In the far field, the first component will create fringes of second harmonic coinciding with those of the fundamental, but its continuous generation, in the absence of propagation of the second component, may be expected to generate fingers, as in the near field of the cosine grating. Given the complex spatial spectrum, it is not surprising that oscillations are not apparent in the amplitude of the fingers, but detailed examination of the field does show that the second harmonic in the fingers has opposite phase from that in the principal fringes. Note that between fringes of the fundamental, its transverse derivative is nonzero, and so Westervelt's argument[5] (see the Introduction) does not deny the existence of fingers.

While the solutions derived above are for simple systems, it may be possible to approximate the boundary condition equation (31) experimentally, by inserting a frequency-dependent attenuator at the intersection of two beams of sound. If the attenuator is thin on the scale $2r_0/K^2$ of the oscillations, and effectively removes the generated harmonics from two intersecting beams, then one would expect a weak far-field finger to be observed.

The analytic solution obtained may also be of use for testing numerical models of nonlinear propagation.

In summary, far from being anomalous, the nonlinear production of harmonic fields in regions where there is little fundamental field is a natural consequence of the imposition of zero amplitude on the harmonics in regions where the fundamental is nonzero, the continuous local production of on-shell harmonics, and suppression of off-shell harmonics.

ACKNOWLEDGMENTS

This research was funded by Engineering and Physical Sciences Research Council Grant No. GR/K28022. The authors are grateful to Professor Sigve Tjøtta for helpful conversations.

[1] V. P. Kuznetsov, ''Equations of nonlinear acoustics,'' Sov. Phys. Acoust. **16**, 467–470 (1971).
[2] J. Berntsen, J. Naze Tjøtta, and S. Tjøtta, ''Near field of a large acoustic transducer. Part IV: Second harmonic and sum frequency radiation,'' J. Acoust. Soc. Am. **75**, 1383–1391 (1984).
[3] J. A. TenCate, ''An experimental investigation of the nonlinear pressure field produced by a plane circular piston,'' J. Acoust. Soc. Am. **94**, 1084–1089 (1993).
[4] C. R. Reilly and K. J. Parker, ''Finite-amplitude effects on ultrasound beam patterns in attenuating media,'' J. Acoust. Soc. Am. **86**, 2339–2348 (1989).
[5] P. J. Westervelt, ''Scattering of sound by sound,'' J. Acoust. Soc. Am. **29**, 934–935 (1957).
[6] J. Berntsen, J. Naze Tjøtta, and S. Tjøtta, ''Interaction of sound waves. Part IV: Scattering of sound by sound,'' J. Acoust. Soc. Am. **86**, 1968–1983 (1989).
[7] Z-Y. Jiang and J. F. Greenleaf, ''The nonlinear interaction of two plane waves in a viscous medium,'' J. Acoust. Soc. Am. **99**, 2783–2790 (1996).
[8] S. Nachef, D. Cathignol, J. Naze Tjøtta, A. M. Berg, and S. Tjøtta, ''Investigation of a high-intensity sound beam from a plane transducer—Experimental and theoretical results,'' J. Acoust. Soc. Am. **98**, 2303–2323 (1995).
[9] J. Naze Tjøtta and S. Tjøtta, ''Interaction of sound waves. Part I: Basic equations and plane waves,'' J. Acoust. Soc. Am. **82**, 1425–1428 (1987).
[10] J. Berntsen, ''Numerical Calculation of Finite Amplitude Sound Beams'' in *Frontiers of Nonlinear Acoustics: Proceedings of the 12th ISNA*, edited by M. F. Hamilton and D. T. Blackstock (Elsevier Science, New York, 1990), pp. 191–196.
[11] A. C. Baker, A. M. Berg, A. Sahin, and J. Naze Tjøtta, ''The nonlinear pressure field of plane, rectangular apertures: Experimental and theoretical results,'' J. Acoust. Soc. Am. **97**, 3510–3517 (1995).
[12] M. A. Foda, ''Nonlinear propagation and distortion of two plane waves interacting at arbitrary angles,'' Acustica **82**, 213–219 (1996).
[13] O. V. Rudenko and S. I. Soluyan, *Theoretical Foundations of Nonlinear Acoustics*, translated from Russian by R. T. Beyer (Consultants Bureau, New York, 1977).
[14] J. Naze Tjøtta and S. Tjøtta, ''Interaction of sound waves. Part III: Two real beams,'' J. Acoust. Soc. Am. **83**, 487–495 (1988).
[15] J. Naze Tjøtta, J. A. TenCate, and S. Tjøtta, ''Effects of boundary conditions on the nonlinear interaction of sound beams,'' J. Acoust. Soc. Am. **89**, 1037–1049 (1991).
[16] C. M. Darvennes and M. F. Hamilton, ''Scattering of sound by sound from two Gaussian beams,'' J. Acoust. Soc. Am. **87**, 1955–1964 (1990).